Chapter-12

Global Positioning System: Theory and Applications

Jagat Dwipendra Ray

Department of Physics, Tezpur University Napaam, 784028 Assam India
E-mail: jogot123@gmail.com

This Chapter gives overview of the space geodetic techniques with special focus on Global Positioning System (GPS). Different segments of GPS, GPS signal, GPS observables and the effect of atmosphere on the signal propagation have been provided in detail. At the end, applications of GPS in various fields have been outlined.

1. INTRODUCTION

Geodesy is the branch of Science, which deals with the measurement and mapping of the Earth's surface. Space Geodesy includes the observational and computational techniques to obtain the solution of several geodetic problems using precise measurements to, from, or between artificial satellites. Space Geodesy seeks solution to the following basic problems in the field of Geodesy:

ISBN: 978-93-85822-38-4

(i) Estimation of precise global, regional and local three-dimensional position
(ii) Mapping of Earth's gravity field
(iii) Measurements and modelling of geodynamical activities like crustal deformation, earth rotation, etc.

The precise measurements of position on Earth's surface and mapping Earth's gravity field attained new heights with the emergence of space geodetic techniques like GPS (Global Positioning System) and GRACE (Gravity Recovery and Climate Experiment). Though GPS is being developed for mainly surveying and navigation, now it is one of the key scientific instruments for studying crustal deformation and atmospheric remote sensing. GRACE, which was launched in 2002 by a joint collaboration of NASA (National Aeronautics and Space Administration) and German Aerospace Centre (DLR), is making detailed measurements of Earth's gravity field which lead to discoveries about spatiotemporal gravity variations and climate change. Along with mapping the Earth's gravity field, GRACE can also be used to study the change in the Groundwater. Apart from GPS and GRACE, the other spaceborne techniques include SAR (Synthetic Aperture Radar), VLBI (Very Long Baseline Interferometer), SLR (Satellite Laser Ranging), LIDAR (Light Detection and Ranging) and DORIS (Doppler Orbitography and Radio positioning Integrated by Satellite) are used in space based geodesy.

The space based geodetic techniques can be classified on the basis of relation between the observation platform and target platform:
(i) Earth to space methods (SLR, GPS, DORIS)

(ii) Space to Earth methods (Radar altimetry, spaceborne laser)

(iii) Space to space methods (GRACE).

In this chapter, we elaborately describe how GPS can be used to monitor geophysical processes, which occur in various spatial and temporal scales [1].

2. GLOBAL POSITIONING SYSTEM (GPS)

The Global Positioning System (GPS) is a satellite based navigation system developed by United States Department of Defence (DoD) in the early 1970s primarily for military purposes. GPS was designed as a ranging system from known positions of navigational satellites in the space to the unknown positions on the Earth [2]. GPS is capable of providing continuous positioning and timing information under any weather condition and anywhere in the world. Owing to its high positioning accuracy, capability of determining velocity and time, availability of signals anywhere in the globe, GPS is being used in numerous applications. The whole GPS system consists of three major segments. The three segments are the space segment (SS), a control segment (CS) and a user segment (US).

ISBN: 978-93-85822-38-4

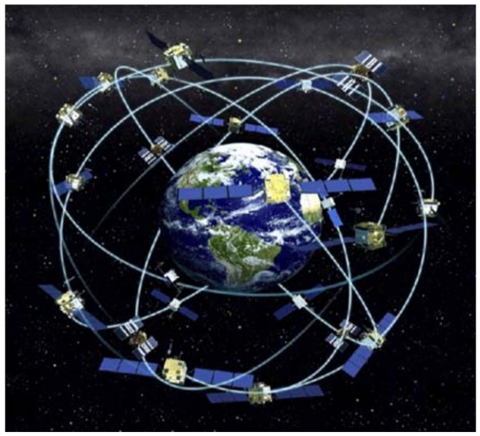

Fig. 1: GPS Navigational Satellites
(Source : https://timeandnavigation.si.edu/satellite-navigation/gps)

(a) Space Segment

The space segment comprises of 24 satellites. As of February 2016, 72 Global Positioning System navigation satellites have been launched that move around the Earth at an altitude of 20,200 km above the Earth's surface in six equally spaced orbital planes with four satellite vehicles(SV) each. The orbital planes have ~55^{o} inclination and are separated by 60^{o}. The orbital period of the Satellite Vehicles is one-half of a sidereal day (11 hours and 58 minutes) so that the satellite passes over the same location almost every day. The whole GPS constellation is arranged in such a way that at least five to eight satellites are always within line of sight from almost everywhere on the Earth.

(b) Control Segment

A worldwide network of tracking stations with a master station (MCS) located in the United States at Colorado Springs, Colorado constitutes the

ISBN: 978-93-85822-38-4

control segment of the GPS system. The sole tasks of the control station are to continuously monitor and control the satellite system, determine the GPS system time, predict the behaviour of the satellite atomic clocks and the satellites ephemerides, and update the navigation message for each particular satellite. The Master Control station uploads ephemerides and clock data to the satellites and then the satellites send subsets of orbital ephemerides data to GPS receivers over the radio signal.

(c) User Segment

The user segment consists of the GPS receivers and the user community. The GPS receivers, tuned to the frequencies transmitted by the satellites is composed of an antenna, receiver-processor and highly stable atomic clock. The GPS receivers convert the satellite signals into position, velocity and time estimates and generally it requires a minimum of four satellites to compute the four dimensions of X, Y, Z (position) and time. With its millimetre level accuracy, GPS is now being widely used in surveying, geodetic control and plate tectonic studies.

2.1 GPS satellite Signal

GPS satellite signal consists of two L-band carrier signals. The two signals are generated by integer multiplication of a fundamental frequency f_o (10.23MHz) by 154 and 120, producing L1 and L2 carrier signals, respectively. These two carrier signals are modulated by two pseudo-random (PRN) noise codes to provide satellite clock reading and information such as orbital parameters. The two PRN codes are the Coarse/Acquisition (C/A) code, which is freely available to the public, and

ISBN: 978-93-85822-38-4

the restricted Precision (P) code, usually reserved for military applications. The Coarse-Acquisition (C/A) code is modulated onto the L1 carrier. The precision (P) code is modulated onto the L1 and L2 carrier signals, which allow for the removal of first order effect of the ionosphere. To prevent any unauthorised use of restricted P code, it was modulated with W code, a special encryption sequence to generate Y-code. The encrypted signal is termed as the P(Y)-code. The GPS signal along with two pseudo-random ranging codes contain navigation message modulated on top of both the C/A and P(Y) ranging codes at 50 bit/s. The navigation message includes satellite ephemerides, satellite clock correction model coefficients, GPS system status information, and ionospheric model.

Table 2.1: Components of GPS signal.

Component	Frequency(MHz)
Fundamental Frequency	f_o=10.23
Carrier L1	154*f_o=1575.42
Carrier L2	120*f_o=1227.60
P Code	f_o=10.23
C/A Code	f_o/10=1.023
Navigation Message	f_o/204600

2.2 GPS Observables

GPS observables are code pseudoranges, phase pseudoranges and Doppler measurements. The pseudorange is the distance between the satellite and the phase centre of the receiver's antenna, which is obtained by calculating the time of transmission of the signal from the satellite to the receiver. The GPS measurements are based on the two clocks used, one in satellite and one in

ISBN: 978-93-85822-38-4

the receiver. Thus, the range measurements are biased by satellite and receiver clock errors and hence the term pseudorange.

(a) Code Pseudorange

Let t^S be the time reading of the satellite clock at which the GPS satellite emits the signal and t_R is the time of reception of the signal at the receiver clock. By denoting the delays of the clocks with respect to GPS systems as δ^S and δ_R, the time shift i.e. the difference between the time readings will be

$$\Delta t = t_R - t^S = [t_R(GPS) - \delta_R] - [t^S(GPS) - \delta^S] = \Delta t(GPS) + \Delta\delta \tag{2.1}$$

The clock bias can be modelled by polynomials of time. The pseudorange is obtained by multiplying the time delay with speed of light c, hence the pseudorange (R) is

$$R = c\Delta t = c\Delta t(GPS) + c\Delta\delta = \rho + c\Delta\delta \tag{2.2}$$

The range ρ is calculated from the signal travel time. The range in other way corresponds to the distance between position of the satellite at epoch t^S (GPS) and the position of antenna of the receiver at epoch t_R (GPS).

(b) Phase Pseudorange

The carrier phase is the measurement of phase difference between received satellite signal and receiver generated carrier phase at the time of reception. The measurement is performed by shifting the receiver generated phase to track the received phase.

Let $\varphi^S(t)$ be the phase of the received signal with frequency $f^S(t)$ and $\varphi_R(t)$ be the phase of the receiver generated carrier wave of frequency f_R. Then

ISBN: 978-93-85822-38-4

$$\varphi^S(t) = f^S t - f^S \frac{\rho}{c} - \varphi_0^S \tag{2.3}$$

$$\varphi_R(t) = f_R t - \varphi_{0R} \tag{2.4}$$

The initial phases φ^S_0 and φ_{0R} caused by clock errors are given by

$$\varphi_0^S = f^S \delta^S \tag{2.5}$$

$$\varphi_{0R} = f_R \delta_R \tag{2.6}$$

Thus, the beat phase is given by

$$\varphi_R^S(t) = \varphi^S(t) - \varphi_R(t)$$

$$= -f^S \frac{\rho}{c} - f^S \delta^S + f_R \delta_R + (f^S - f_R)t \tag{2.7}$$

The difference of the frequencies f^S, f_R from the nominal frequency f is only in the range of fractional parts of Hz and thus putting f for f^S, f_R we get

$$\varphi_R^S = -f \frac{\rho}{c} - f\Delta\delta \tag{2.8}$$

Where $\Delta\delta = \delta^S - \delta_R$. The number of integer carrier waves N (integer ambiguity) between the receiver and the satellite cannot be measured and varies for every satellite-receiver combination but receiver can measure the fractional phase. The integer ambiguity (N) remains constant if there is no loss of connection between receiver and satellite but the fractional beat phase keep changing with time. The beat phase is given by

$$\varphi_R^S(t) = \Delta\rho_R^S(t, t_0) + N \tag{2.9}$$

ISBN: 978-93-85822-38-4

Where $\Delta\varphi_R^S$ denotes the fractional phase at epoch t. Substituting Equation (2.9) into Equation (2.8) and using $\Phi = -\Delta\rho_R^S$, $f = \dfrac{c}{\lambda}$ the phase pseudorange can be written as

$$\Phi = \frac{1}{\lambda}\rho + \frac{c}{\lambda}\Delta\delta + N \tag{2.10}$$

(c) Doppler measurements

The Doppler measurement is a measure of the instantaneous phase rate, which is made in the phase lock loop. Basically it is used for velocity estimation. The Doppler measurement equation is given by

$$D = \lambda\,\dot{\varphi} = \dot{\rho} + c\Delta\dot{\delta} \tag{2.11}$$

2.3 Atmospheric Effect on GPS Signal

When the GPS signal propagates through atmosphere it gets refracted causing delays in the path of the signal propagation. The signal gets delayed by the interaction with the charged particles of the ionosphere and humidity of the troposphere. Below, we give an account of these two kinds of atmospheric effects on GPS positioning.

(a) Ionospheric Effect

The ionosphere is shell of electrons and electrically charged atoms and molecules that surrounds the Earth, extending from about 50 to 1000 km. Radio wave when passes though the ionized plasma, get affected by with a characteristic modification of wave parameters such as amplitude, phase of polarization [3-4]. The GPS signal when travels through the Ionosphere suffer a propagation delay. The propagation delay can be obtained by

ISBN: 978-93-85822-38-4

considering the nature of the refractive index which depends on the content of the ionospheric plasma [5]. The refractive index of the ionosphere is not equal to that of the free space, due to which the speed of the radio wave differs from its speed in the free space [5]. Also, spatial variations of the refractive index cause a curvature in the propagation path. Both these effects altogether impose a delay or phase advance of the satellite navigational signal like GPS. The group delay and Phase advance are equal in magnitude and opposite in sign. The variation of the ionospheric impact is larger than tropospheric effects [5]. The amount of ionospheric delay or phase advance of the GPS signal can fluctuate from a few meters to more than twenty meters in a day. Due to the complex interactions between geomagnetic field and solar activities, it is very difficult to model the ionospheric effects. On the other hand, the ionosphere is a dispersive medium and hence the magnitude of the ionospheric delays depends upon the frequency of the signal. GPS system is designed with two carrier frequencies, so that ionospheric effects can be removed by computing the frequency dependent delay. Ionospheric effects on the carrier phase of GPS L1 signal can be expressed (in meters) as

$$\varphi_1 = \rho + N_1\lambda_1 - \frac{40.3\int N_e dL}{f_1^2} - \frac{1.1284\times 10^{12}\int N_e B\cos\theta .dL}{f_1^3} - \frac{812.47\int N_e^2 dL}{f_1^4}$$

(2.12)

where ρ is the geometric range between the satellite and the GPS receiver, λ_1 is the wavelength, N_1 is the integer ambiguity, N_e is the free electrons per unit volume, L is the path length, B is the magnetic field and θ is the

ISBN: 978-93-85822-38-4

angle between GPS signal and magnetic field. Similar expression (2.12) apply for GPS L2 signal with frequency f_2 [6]. The first, second and third order ionospheric refraction terms can be described as :

$$1^{st}\text{ order} = \frac{-40.3\int N_e dL}{f_1^2} \tag{2.13}$$

$$2^{nd}\text{ order} = \frac{-1.1284\times 10^{12}\int N_e B\cos\theta . dL}{f_1^3} \tag{2.14}$$

$$3^{rd}\text{ order} = \frac{-812.47\int N_e^2 dL}{f_1^4}. \tag{2.15}$$

(b) Tropospheric Effect

The neutral layer of the Earth's atmosphere extending from Earth's surface up to about 50 km. The effect of the neutral atmosphere on signal propagation is conventionally called as Tropospheric effect. The troposphere is a non-dispersive medium with respect to radio signal up to frequencies up to 15GHz and therefore tropospheric effects on the propagation of GPS signal is independent of frequency. Electromagnetic waves are get affected by neutral atoms and molecules of the neutral atmosphere and the effect is termed as tropospheric refraction or tropospheric delay. The amount of the tropospheric delay reaches up to 2m in the zenith and increases with the increase of the sight line to the satellite. Due to the variable refractive index along the path of propagation, GPS signal affected by two ways: First, as the refractive index is not equal to that

ISBN: 978-93-85822-38-4

of the free space, the velocity get lowered; secondly the signal travel in a curved path instead of straight line. The time delay of the signal can be described in terms of an equivalent increase in travel path length.

The tropospheric excess path length is given by

$$\Delta L_{Trop} = \int_L n(s)ds - G \tag{2.16}$$

where $n(s)$ is the refractive index as a function of position s along the curved path L and G is the direct path, which would occur in the absence of the atmosphere. Equation (2.16) can be re-written as

$$\Delta L_{Trop} = \int_L [n(s)-1]ds + [S-G] \tag{2.17}$$

where S is the path length along L. Equation (2.17)) describes the total delay caused by troposphere. The first term is due to the slowing of the velocity and the second term [S-G] is due to the bending which represents the difference in the distance between the straight line path G (that a radio-wave could follow in the absence of atmosphere) and the real curved path S and it is called geometrical error. When the signal followed straight path and there is no horizontal gradients of refractive index, the bending term [S-G] vanishes. As the GPS signal in the atmosphere propagate just slightly slower than in a vacuum, the refractive index is expressed by the term refractivity

$$N_{Trop} = 10^6(n-1) \tag{2.18}$$

so that Equation (2.17) becomes

$$\Delta L_{Trop} = 10^{-6}\int_L N_{Trop}ds \tag{2.19}$$

ISBN: 978-93-85822-38-4

According to Hopfield [1969] [7] refractivity can be separated into a dry or hydrostatic and wet component

$$N_{Trop} = N^{d}_{Trop} + N^{w}_{Trop} \tag{2.20}$$

where dry part is due to dry atmosphere and wet part is mostly from water vapour. Therefore tropospheric delay can be expressed as the sum of hydrostatic as well as wet components

$$\Delta L_{Trop} = \Delta L^{d} + \Delta L^{w} \tag{2.21}$$

or

$$\Delta L_{Trop} = 10^{-6}\int_{L} N^{d}_{Trop}\, ds + 10^{-6}\int_{L} N^{w}_{Trop}\, ds \tag{2.22}$$

Tropospheric delay, at the zenith direction is about 2.5 m [8]. 90% of the tropospheric delay arises from the hydrostatic or dry delay and about 10% from the wet delay [9].

2.4 Theory of GPS data processing using GAMIT/GLOBK

The GPS data have been processed by using GAMIT/GLOBK, a comprehensive GPS analysis package developed at MIT, the Harvard-Smithsonian Center for Astrophysics (CfA), Scripps Institution of Oceanography (SIO), and Australian National University for estimating station coordinates and velocities, stochastic or functional representations of post-seismic deformation, atmospheric delays, satellite orbits, and Earth orientation parameters [10]. The software makes use of C-shell scripts which are stored in /com to control the processing, which invoke the FORTRAN programs compiled in the /libraries, /gamit, and /kf directories. The software is made to run under any UNIX operating system supporting

ISBN: 978-93-85822-38-4

X-windows. The primary phase processing is performed by GAMIT which loosely stands for GPS analysis at MIT and it produces associated covariance matrix (quasi observables). The quasi-observables are combined using GLOBK (Global Kalman Filter). We stabilized the solution in a uniform reference by applying generalised constraints for better realization of the reference frame. We first provide theory about the analysis of primary observation (Phase Processing), combination using quasi-observation and imposition of generalised constraints. The mathematical framework is based on four-dimensional integrated geodesy, which embodies the intrinsic correlation between the Earth's shape and the gravitational potential [11-12].

(a) Analysis of Primary observations

The geodetic displacement l(t) can be expressed as

$$l(t) = FX(a,t), U(X(a,t)), h(t) \tag{2.23}$$

where, X(a,t) is the position vector, whose time dependency is given by the parameter a; U(X(a,t)) is the reference gravitational potential; h(t) are auxiliary parameters which represent propagation effects, satellite positions, etc.; and F is non-linear function which operates upon X, U and h to produce value of l(t).

The linearised observation equation can be written as

$$\delta l = \left(\frac{\partial F}{\partial X} + \frac{\partial F}{\partial U}\frac{\partial U}{\partial X} \right) \Delta X(a,t) + \frac{\partial F}{\partial U}\Delta U(X_0) + \frac{\partial F}{\partial h}\Delta h_0 + \varepsilon \tag{2.24}$$

where δl represents the residual between observed and calculated displacement, based on *a priori* model; $\Delta X(a,t)$ is the adjustment of time

ISBN: 978-93-85822-38-4

dependent position vector; $\Delta U(X_0)$ is the correction to the reference potential at an initial position ; Δh_0 is the correction of the parameter h_0 and ε denotes errors in the observations. The term $\Delta X(a,t)$ carries the information about crustal deformation[13] and treated as quasi observation. The quasi-observation has the all geodetic information in a compressed form and GAMIT saves it as an h-file.

(b) Combination of the quasi-observables

Although classical least squares and stochastic estimators are natural platform for combining data from multiple epochs and different types of observations but for generality the quasi-observations have been combined using Kalman filter. Taking $\delta l_k = l_k - l_{0k}$ as the vector of linearized quasi-observations at time t_k , where l_{0k} represents the *a priori* values and l_k are the estimates of quasi observables from GAMIT analysis. The observation equation is $l_k = A_k \delta x_k + \varepsilon_k$, where x_k are the parameters to be estimated and A_k is the design matrix. Observation equation from two different subsets of data can be combined using Kalman filter with assumption that data are uncorrelated to each other and the uncertainties are purely white. The observation equation for the two subsets

$$\delta l_1 = A_1 \delta x_1 + \varepsilon_1 \tag{2.25}$$

$$\delta l_2 = A_2 \delta x_2 + \varepsilon_2 \tag{2.26}$$

with the associated covariance matrix C_1 and C_2; the solution of the combination is given by

ISBN: 978-93-85822-38-4

$$\delta x_{12} = C_{12}(A_!^T C_1^{-1}\delta l_1 + A_2^T C_2^{-1}\delta l_2 \qquad (2.27)$$

Where, $C_{12} = \left(A_1^T C_1^{-1} A_1 + A_2^T C_2^{-1} A_2 + C_x\right)^{-1}$ is the covariance matrix of the combined solution, C_x is the covariance matrix of the a priori values of the parameters x. The misfit to the data aregiven by weighted sum of squared residuals $\left(X^2\right)$,

$$X_{12}^2 = \left(\delta l_1 - A_1\delta_{12}\right)^T C_1^{-1}(\delta l_1 - A_1\delta x_{12}) + (\delta l_2 - A_2\delta x_{12})^T C_2^{-1}(\delta l_2 - A_2\delta x_{12}) \qquad (2.28)$$

The weighted sum of squared residuals $\left(X^2\right)$is widely used to rescale the a posteriori uncertainty, to detect observation blunders, to test the compatibility of different data sets, and to assess the significance of different parameterizations [14]. These steps have been implemented in GLOBK programme to combine the quasi-observables.

(c) Imposing General constraints

The GPS satellites although provide a natural dynamic frame for ground-based geodesy, the doubly differenced phase observations do not tie a ground station to the orbital constellation at the millimetre level which we require for scientific studies. For meaningful analysis of the position and rate estimates from a GPS network solution, it is mandatory to express the solution in suitable reference frame, which can perfectly describe the position and rate estimates. A precise and rigorous reference frame is realized by imposing generalized constraints, in which we minimize the

ISBN: 978-93-85822-38-4

adjustments of ordinates of frame defining sites using sequential Kalman filter. The step is performed by GLORG programme of GLOBK.

Let the parameter adjustments before the constraints are δx_c with covariance C_x and misfit X_x^2; the updated solutions after imposing constraints become

$$\hat{x} + C_x A_c^T (C_c + A_c C_x A_c^T)^{-1} (l_c - A_c \delta\hat{x}) \tag{2.29}$$

$$C_c = C_x - C_x A_c^T (C_c + A_c C_x A_c^T)^{-1} A_c C_x \tag{2.30}$$

$$X_c^2 = X_x^2 + (l_c - A_c \delta\hat{x})^T (C_c + A_c C_x A_c^T)^{-1} (l_c - A_c \delta\hat{x}) \tag{2.31}$$

GLORG performs this frame defining sites by estimating 7 Helmuert transformation parameters (3 translation, 3 rotation and 1 scale factor) which allows the reference sites to adjust freely thereby revealing bad data or coordinates. Frame realized by using two different sets of reference frames will differ only in estimated Helmuert parameters without any internal distortion. Another approach is to impose finite constraint which is rarely used practice no a days as it can distort the network if the assigned constraints are not correct for the a priori coordinates and data [12].

2.5 GPS Applications

(a) In Geophysics

GPS is widely used to monitor various geophysical phenomena specially in studying crustal deformation though comparing the observed and modelled movement of the Earth's surface [15]. The observed surface displacement contains contribution from varieties of geophysical phenomena with different spatial and temporal scales [16]. The effect of various physical

ISBN: 978-93-85822-38-4

sources can be modelled by analysing the GPS derived position time series with different time length and resolution. The signal of co-seismic displacements [17-18], seismic waves [19], volcanism [20] which generally last for couple of minutes and can be studied by short and high sampling GPS data. Investigation about deformation due to elastic surface mass loading require long time series having daily or weekly samples. GPS time series having different time scales ranging from seconds to decades can be applied to study all phases of earthquake cycle [21].

(b) In Atmosphere and Hydrology

The delay of the GPS signal caused by troposphere and ionosphere is used to estimate atmospheric perceptible water vapor (PWV) and ionospheric total electron content (TEC). GPS with low operational cost, all weather capability and high temporal resolution provide attractive solution for PWV estimation. GPS meteorology has procured wide application in weather forecasting [22-25] and study of severe weather condition [26-31].The TEC measurements attained from dual frequency GPS receivers are one of the most important methods of studying the ionosphere. GPS derived TEC can be used to investigate earth –ionosphere coupling as ionospheric electron suffers anomaly due to strong earthquake. Detection of pre-seismic ionospheric TEC enhancement opened a new hope for using GPS TEC [32] as a precursor for detecting earthquake.

GPS technology has also been successfully used in measuring surface soil moisture [33], snow depth [34] and in geodetic measurements of detecting elastic response of the Earth due to hydrological changes [35-37]. The presence of hydrological signal in GPS geodetic time series is validated by using either hydrological models[38] or through GRACE satellite measurements [39-42]. Generally it is the vertical displacements that are used to constrain the effect of hydrological signal, however horizontal displacement can also be used to locate the hydrological loading sources [43-44]. Recently GPS derived time series is applied as an independent tool to estimate terrestrial water storage [45].

An overview avout GPS has been presented in this chapter. GPS is composed of three segments namely (i) Space segments, (ii) Control Segment and (iii) User Segment. We briefly described each of the segments in this chapter. There are three GPS observables viz. Code pseudorange, Phase pseudorange and Doppler measurements. GPS signal when travelled through the atmosphere suffers refraction which in turn causes signal delay. Effects of ionospheric refraction and tropospheric refraction have been provided in this chapter. Theoretical background of the GAMIT/GLOBK software, which has been used to process the GPS raw data, is also provided. The theory of GPS data processing can be divided into three steps: (i) Analysis of primary observation, (ii) Combination of quasi-observables and (iii) Imposition of generalized constraints.

REFERENCES

[1] Chen, Q. Ph.D. Thesis, University of Stuttgart at Stuttgart, Germany, 2015.
[2] Hofmann-Wellenhof, B., Lichtenegger, H. & Collins, J., Springer, Wien (Austria),1997.
[3] Budden, D. Cambridge University Press, Cambridge, 1985.
[4] Davies, K. Ionospheric Radio, Peter Peregrinus Ltd.,London, UK,1990.

ISBN: 978-93-85822-38-4

[5] Hoque,M.M., & Jakowski, N., in *Global Navigation Satellite Systems: Signal, Theory and Applications*, S Jin et. al, eds., InTech, Neustrelitz,2012, 381-404

[6] Petrie, E.J., Hernández-Pajares, M., Spalla, P., Moore, P., & King, M.A. *Surveys in Geophysics* **32**(3),197-253,2011.

[7] Hopfield, H.S. *Journal of Geophysical research* **74**(18), 4487-4499, 1969.

[8] Ahn, Y.W. Master Thesis*,* University of Calgary at Calgary, Canada, 2005.

[9] Janes, H.W., Langley, R.B., & Newby, S.P. *Bulletin géodésique* **65**(3), 151-161.1991.

[10] Herring, T.A., King, R.W., & McClusky, S.C.1-48,2010.

[11] Hein, G.W., in *Mathematical and Numerical Techniques in Physical Geodesy SE - 9*, Sünkel, H. ed., Springer Berlin Heidelberg, 1986, 505–548.

[12] Collier, P.A., Eissfeller, B., Hein, G.W., & Landau, H., *Bulletin géodésique* **62**(1), 71-91,1988.

[13] Dong, D., Herring, T.A., & King, R.W, *Journal of Geodesy* **72**(4),200-214,1998.

[14] Segall, P., & Matthews, M.V, *Journal of Geophysical Research*, **93**(B12), 14954-14966, 1988.

[15] Blewitt, G, in *Treatise on Geophysics,* G. Schubert eds.,Oxford: Elsevier,2007,307-338.

[16] Chen, Q. Ph.D. Thesis, University of Stuttgart at Stuttgart, Germany, 2015.

[17] Larson, K.M., Bodin, P., & Gomberg, J. *Science* **300**(5624), 1421-1424.2003.

[18] Hsieh, C-S., & Shih, T-Y.*Terrestrial, Atmospheric and Oceanic Sciences* **17**(3),517-532,2006.

[19] Kouba, J. *Studia Geophysica et Geodaetica* **47**(4), 741-755, 2003.

[20] Ji, K.H., & Herring, T.A. *Geophysical Research Letters* **38**(6), L06307,2011.

[21] Prawirodirdjo, L., McCaffrey, R., Chadwell, C.D., Bock, Y. , & Subarya, C. *Journal of Geophysical Research: Solid Earth* **115**(B3), B03414,2010.

[22] Bordi, I., Fraedrich, K., Sutera, A., & Zhu, X. *Theoretical and applied climatology* **115**(3-4),615-625,2014.

[23] Gutman, S.I., & Benjamin, S.G. *GPS solutions* **4**(4), 16-24, 2001.

[24] Hagemann, S., Bengtsson, L., & Gendt, G. *Journal of Geophysical Research: Atmospheres* **108** (D21), 4678,2003.

[25] Rocken, C., Ware, R., Van Hove, T., Solheim, F., Alber, C., & Johnson, J. *Geophysical Research Letters* **20**(23), 2631–2634,1993.

[26] Choy, S., Wang, C., Zhang, K., & Kuleshov, Y. *Advances in Space Research* **52**(9), 1688-1699,2013.

[27] Hodges, K.I., Hoskins, B.J., Boyle, J., & Thorncroft, C. *Monthly Weather Review* **131**(9), 2012-2037, 2003.

[28] Liou, Y.A. , & Huang, C.Y. *Earth, planets and space* **52**(10), 709-712,2000.

[29] Seko, H., Nakamura, H., Shoji, Y., & Iwabuchi, T. *Journal of the Metereological Society of Japan* **82**(1B),569-586,2004.

[30] Wang, H., Wei, M., Li, G., Zhou, S., & Zeng, Q. *Advances in Space Research* **52**(4),656-667,2013.

[31] Xie, F., Wu, D.L., Ao, C.O., & Mannucci, A.J. *Atmospheric Chemistry and Physics*, **10**(14), 6889-6899, 2010.

[32] Heki, K. *Geophysical Research Letters* **38**(17), L17312,2011.

[33] Larson, K.M., Small, E.E., Gutmann, E.D., Bilich, A.L., Braun, J.J., & Zavorotny, V.U. *Geophysical Research Letters* **35**(24), L24405, 2008.

[34] Larson, K.M. and Nievinski, F.G. GPS snow sensing: results from the EarthScope Plate Boundary Observatory, *GPS solutions* **17**(1), 41-52, 2013.

[35] Van Dam, T., Wahr, J., Milly, P.C.D., Shmakin, A.B., Blewitt, G., Lavallée, D., & Larson, K.M. *Geophysical Research Letters* **28**(4),651-654,2001.

[36] Bevis, M., Kendrick, E., Cser, A., & Smalley, R. *Physics of the earth and Planetary Interiors* **141**(2), 71-78,2004.

[37] Bevis, M., Alsdorf, D., Kendrick, E., Fortes, L.P., Forsberg, B., Smalley, R., & Becker, J. , *Geophysical research letters* **32**(16),L16308,2005.

[38] Döll, P., Kaspar, F., & Lehner, B . Journal *of Hydrology* **270**(1), 105-134, 2003.

[39] Van Dam, T., Wahr, J., & Lavallée, D. *Journal of Geophysical Research: Solid Earth* **112**(B3), B03404,2007.

[40] Tregoning, P., Watson, C., Ramillien, G., McQueen, H., & Zhang, J. *Geophysical Research Letters* **36**(15), L15401,2009.

[41] Tesmer, V., Steigenberger, P., van Dam, T., & Mayer-Gürr, T. *Journal of Geodesy* **85**(5),291-310,2011.

[42] Fu, Y., & Freymueller, J.T. *Journal of Geophysical Research: Solid Earth* **117**(B3), B03407,2012.

[43] Wahr, J., Khan, S.A., Dam, T., Liu, L., Angelen, J.H., Broeke, M.R., & Meertens, C.M. *Journal of Geophysical Research: Solid Earth* **118**(4), 1795-1806,2013.

[44] Fu, Y., Argus, D.F., Freymueller, J.T., & Heflin, M.B. *Geophysical Research Letters* **40**(23), 6048-6053,2013.

[45] Fu, Y., Argus, D.F., & Landerer, F.W *Journal of Geophysical Research: Solid Earth* **120**(1),552-566, 2015.

ISBN: 978-93-85822-38-4